SIMULATION AND MEASUREMENT OF X-RAY SCATTERED RADIATION IN RADIODIAGNOSIS

by

Xian Qiang TANG [1,2], ***Rui ZHAO*** [2], ***Wei Feng ZHU*** [1,2], ***Bin GUO*** [2], ***Feng QIN*** [2,3], ***Bo LIU*** [2], ***and Jin Jie WU*** [1,2*]

[1] Chengdu University of Technology, Chengdu, China
[2] National Institute of Metrology, Beijing, China
[3] China Jiliang University, Hangzhou, China

Scientific paper
https://doi.org/10.2298/NTRP2302125T

This work aims to measure the scattered radiation energy spectrum and radiation dose at different positions during radiological diagnosis through the Monte Carlo simulation and experiment. The results show that the average energy of the scattered radiation energy spectrum increases with the increase of the tube voltage and decreases with the increase of the scattering angle, but it changes very little with the measuring distance. It is not unified for the scattered radiation distribution in the space around the water phantom at the same tube voltage, and the exposure to scattered radiation is greater on the side closer to the water phantom or the X-ray tube. This indicates that the radiation exposure is not unified for medical staff in the scattered radiation field. The scattering energy spectrum and dose distribution are helpful to evaluate the scattered radiation exposure and enhance the self-protection awareness of medical staff in practice.

Key words: radiodiagnostic X-ray, scattered radiation, Monte Carlo, energy spectra, radiation exposure

INTRODUCTION

With the development of modern medicine, diagnostic radiology plays an increasingly important role in medicine. The examination time is increasing in neuroradiological, cardiological and orthopedics using X-ray fluoroscopy [1, 2]. As an important means of disease diagnosis, computed tomography (CT) is used more and more frequently. The use of X-ray will inevitably lead to the increase of radiation exposure of medical staff, which increases the risk of radiation damage. Research shows that the risk will increase for a brain tumor, melanoma and breast tumor in the long-term exposure to low levels of an effective dose [3]. In 2011, the International Committee on Radiological Protection (ICRP) further adjusted the annual dose limit for the eye lens, which was reduced from 150 mSv to 20 mSv [4]. This reduction of the annual dose limit is to prevent the occurrence of cataract caused by radiation damage to the lens. Some studies have shown that long-term radiation exposure may lead to cataract formation, because cataractogenesis is not a long-term assumed deterministic effect but tends to be a stochastic effect [5]. As the annual dose limit of the eye lens is greatly reduced, a large number of medical staff will probably exceed this limit. The results of Sanchez *et al*. [6] indicate that more than 50 % of radiologists received doses higher than the dose limit of 20 mSv per year from 2004 to 2010. This means that we could better perform dose monitoring to avoid underestimating the dose received by medical staff after understanding the scattered radiation exposure of medical staff.

In the past, there have been many studies about scattered radiation exposure in radiological diagnosis. In 1996, Marshall *et al.* [7] used the Monte Carlo method to simulate the scattered X-ray energy spectrum of patients in radiological diagnosis, and obtained the scattering energy spectrum of the X-ray tube above and below the patient couch. In 1997, Fehrenbacher *et al*. [8] measured the average energy of the scattered X-ray energy spectrum in radiological diagnosis and found that the average energy decreased toward the X-ray tube side regardless of any tube voltage. In 2019, Masterson *et al*. [9] measured the scattered X-ray energy spectrum in therapeutic radiology and studied the relative response of dosemeters to changes in the scattering energy spectrum.

In radiation medicine, the radiation exposure for medical staff is mostly due to scattered radiation from patients [10, 11]. The efficiency of scattered radiation protection for medical staff mainly depends on whether the protective equipment is worn properly and the size of the scattered radiation in the space.

* Corresponding author, e-mail: wujj@nim.ac.cn

Antić [12] proposed a new method of installing protective screens, which is more reliable and effective for scattered radiation protection.Therefore, enhancing the understanding of the scattered radiation field is beneficial to enhance the efficiency of scattered radiation protection.

In this study, the scattering energy spectrum in the direction of the 90° scattering angle and the scattering dose at different scattering angles are measured. In addition, the distribution of the scattering energy spectrum in the space around the water phantom is also obtained through the Monte-Carlo program. The information of scattered radiation distribution is explored in radiological diagnosis through experiment and simulation. The result could help medical staff to evaluate the scattered radiation exposure during the practice and ensure reduction of unnecessary irradiation.

PRINCIPLE AND METHOD

Measurement devices and materials

The filtration X-ray spectrum is generated with a COMET MXR-320/26 X-ray tube, which has a tungsten anode with an angle of 20° and inherent filtration of 3 mm of beryllium. The high voltage was provided by two 160 kV and 45 kHz high-frequency generators. The X-ray is collimated through a beam limiting aperture made with lead, where the primary beam limiting aperture has a diameter of 1.9 cm and a thickness of 2 cm. The collimated X-ray forms a uniform radiation field at the reference plane, where the diameter of the uniform radiation field is 9 cm at 1 m from the focal spot. In addition, the detector is positioned with multiple lasers. The cylindrical water phantom was used as a scattering medium with a diameter of 20 cm and a height of 20 cm [13], and the center of the water phantom is 100 cm from the tube focus. The experimental set-up is shown in fig. 1.

The scattered radiation dose was measured through a standard ionization chamber detector TW 34069 (PTW, Freiburg, Germany). The sensitive volume was 6 cm^3 and connected to the outside air. The X-ray measurement of the ionization chamber ranges from 25 keV to 150 keV, and its energy response is less than 4 % within the measurement range, and the value is traced to the X-ray air kerma standard. Three directions of 60°, 90°, and 120° with the incident X-ray radiation were selected for measurement under the condition of 80 kV, 100 kV and 120 kV. The scattered radiation doses were obtained at 30 cm, 45 cm and 60 cm from the center of the water phantom in each direction.

A portable X-123 CdTe spectrometer detector (Ametek-Ortec, PA, USA) with a sensitive volume size of 5 mm × 5 mm × 1 mm is used for measuring the scattering energy spectrum. It is a high performance X-ray and gamma-ray detector with an energy resolution of less than 1.5 keV full width at half maximum (FWHM) at ^{57}Co (122 keV). The collected pulse signals are processed by a DP5 digital pulse processor, which has the advantages of better resolution, higher count rate and better stability than the shaping amplifier and multi-channel analyzer (MCA) in most analog systems. To reduce the photon fluence and prevent saturation of the detector during measurement, a 3 mm aperture lead pinhole collimator was used to collimate the detector. The CdTe detector was placed in the direction of 90° with the incident X-ray radiation direction. The tube voltage was set at 80 kV, 100 kV and 120 kV, and the tube current was 0.5 mA. The scattering spectra were measured at 30 cm, 45 cm, and 60 cm from the center of the water phantom.

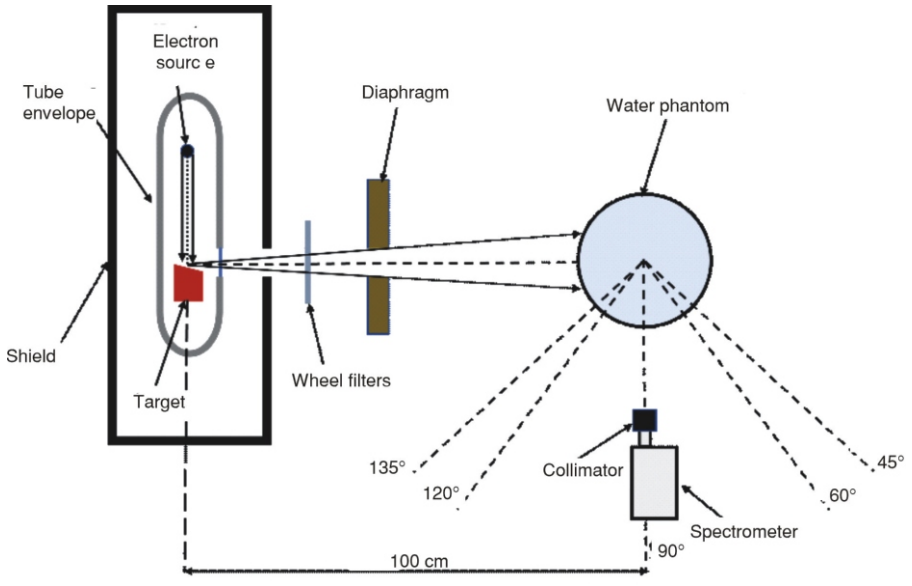

Figure 1. Diagram of the experimental set-up

Monte-Carlo simulation

Geant4 is a Monte Carlo toolkit for simulating radiation transmission, which is mainly used for simulation of particles' interaction and transport in high energy physics, medical physics, space research, and many other fields [14]. The diagnostic X-ray scattered radiation simulation was constructed based on a medical procedure framework in Geant4 to simulate the scattered radiation in the surrounding environment after the incident X-ray reacts with a water phantom. In order to reduce the simulation time and increase the detection efficiency, the X-ray energy spectra of 80 keV, 100 keV and 120 keV were used as input sources. The physical list in the simulation uses the official QBBC provided by Geant4, which includes the photoelectric effect, Compton scattering and Rayleigh scattering. The cylindrical water phantom with a diameter of 20 cm and height of 20 cm was used as a scattering medium, which was composed with a thickness of a 0.5 cm polymethyl methacrylate (PMMA) wall and a water filled inner layer. It is placed at a distance of 100 cm from the particle source with the center on the same horizontal line as the particle source. In order to obtain the scattered radiation around the water phantom, the measurement positions were set at different angles (45°, 60°, 90°, 120°, and 135°) and different distances (30 cm, 45 cm, 60 cm, and 100 cm). A circular plane with a diameter of 30.4 mm was constructed at each measurement position, and the momentum of scattered photons across the plane was recorded to obtain the scattering energy spectrum. The mean energy of the scattering energy spectrum was calculated [15].

The mean energy of the X-ray is calculated by

$$\overline{E} \quad \frac{\int_0^{E_{\max}} \Phi_E E \mathrm{d}E}{\int_0^{E_{\max}} \Phi_E \mathrm{d}E} \tag{1}$$

where Φ_E is the total fluence of the photon with energy between 0 and E, and E – the energy.

Figure 2 shows the positional relationship between the medical staff and the patient, which is the experimental results and explain the correspondence between the experiment and the actual situation. The measurement distance of the water phantom scattering angle 90° direction is equivalent to the distance between the medical staff and the patient during the study. The scattering angle from the 45° to 90° direction corresponds to the upper body space of the medical staff, and from 90° to 135° the direction corresponds to the lower body space. The X-ray tube is located below the patient's couch.

The X-ray radiation qualities

The beam quality of an X-ray machine depends on the total filtration during the irradiation process, which includes intrinsic and additional filtering. Inherent filtration helps to absorb the low energy part of the

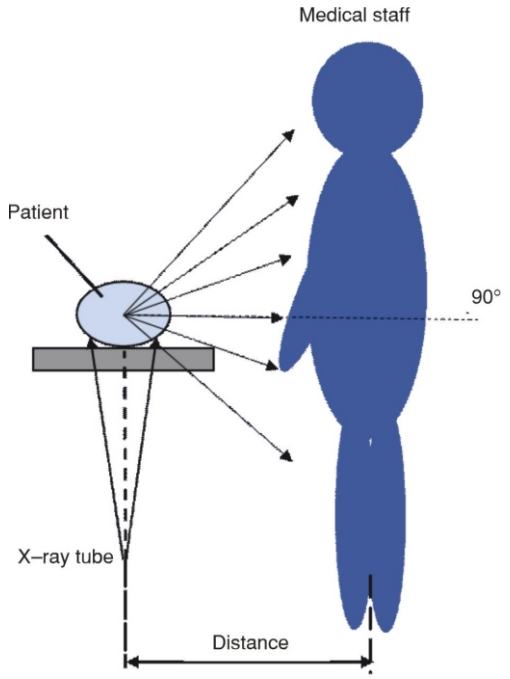

Figure 2. Diagram of the location between medical staff and patients

X-ray beam when passing through the X-ray tube. This absorption occurs in the oil, glass, window and other parts of the X-ray tube, which is determined by the characteristics of the X-ray machine itself. The function of additional filtering is to adjust the filtered X-ray energy spectrum distribution to obtain the required radiation quality. The ASTM Standard F2547-06 recommends the use of tube voltages from 60 kV to 130 kV for radiation attenuation measurements, as they span the energy range used for medical X-ray imaging, excluding mammography. This experiment was conducted under the X-ray lead equivalent reference radiation [16]. Three radiation qualities of tube voltage 80 kV, 100 kV, and 120 kV were selected to measure the scattering energy spectrum and scattering dose.

RESULTS AND DISCUSSION

Results of the measured and simulated scattered radiation energy spectrum

The characteristics of the spectrometer used need to be determined before measuring the scattering energy spectrum. The results of the study indicate that detectors may be too sensitive to photon fluence or may not have sufficient energy resolution [17, 18], while those suitable detectors may be expensive or bulky, resulting in the inability to use suitable detectors in experiments. The sensitivity of the detector to photon fluence is affected by its pulse-counting capability. If the detector wants to record two independent photons during measurement, there needs to be enough time delay between the two events to ensure that the two pulses do not combine into one pulse or

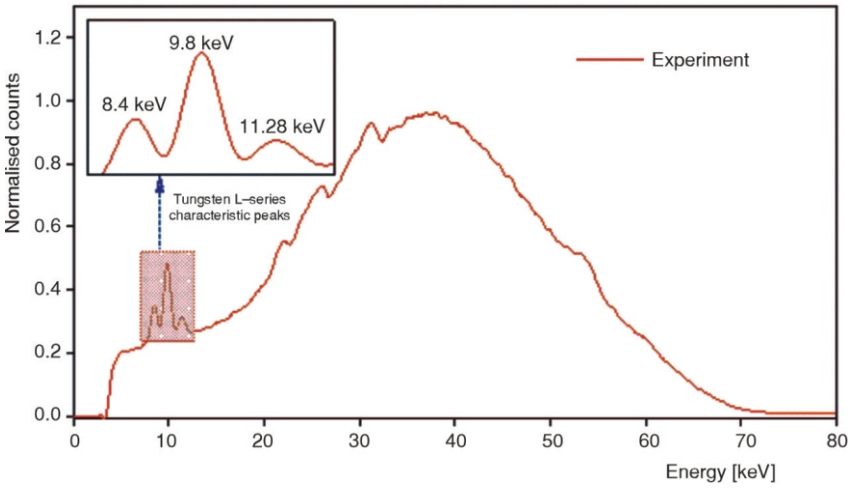

Figure 3. Scattering energy spectrum without additional filtering under 80 kV

lose the second pulse while the first pulse remains unchanged. However, if the second event occurs before all the charges of the first event are collected the semiconductor detectors, the carriers generated by the second event will be added to the pulses generated by the initial event, resulting in no difference between pulse stacking and dead time [19]. The fast channel pulse resolution time of the DP5 digital pulse processor reaches 120 ns in the experiment. When detecting the scattering energy spectrum, a collimator with a 3 mm aperture was added in front of the detector to reduce the intensity of photons reaching the detector surface to prevent saturation of the detector. The dead time of the final detection was less than 3 %, which meets the requirements of the experiment.

Firstly, the scattering energy spectrum was measured and simulated at different distances (30 cm, 45 cm, and 60 cm) from the center of the water phantom at a scattering angle of 90°. Due to the collimator of the spectrometer, there is no need to consider secondary radiation from the floor, walls, and ceiling, nor leakage radiation from the X-ray tube during the measurement process. However, when measuring the scattering energy spectrum, it is difficult to keep the scattered X-rays in the same horizontal line with the collimator aperture and the detector. The scattered X-ray is obliquely incident on the collimator and passes through the edge of the aperture resulting in distortion of the measured scattering energy spectrum [17]. At the same time, there is an L-series characteristic peak of tungsten in the incident energy spectrum, which affects the low energy part of the measured energy spectrum. Figure 3 shows the scattering energy spectrum without additional filtering at a voltage of 80 kV at a measurement distance of 60 cm. There is no need to consider the secondary radiation of the surrounding environment and collimator, as well as the L-series characteristic peaks of tungsten, and the ideal photon fluence spectrum is ultimately obtained. The measured and simulated spectral data at the same measurement distance are normalized and compared, and the trends of the two were in good agreement, which indicates the correctness of the established detection scattering energy spectrum model. At the same time, it is also observed that with the increase of tube voltage, the characteristic peaks in the scattering energy spectrum are more obvious. Figure 4 shows the normalized

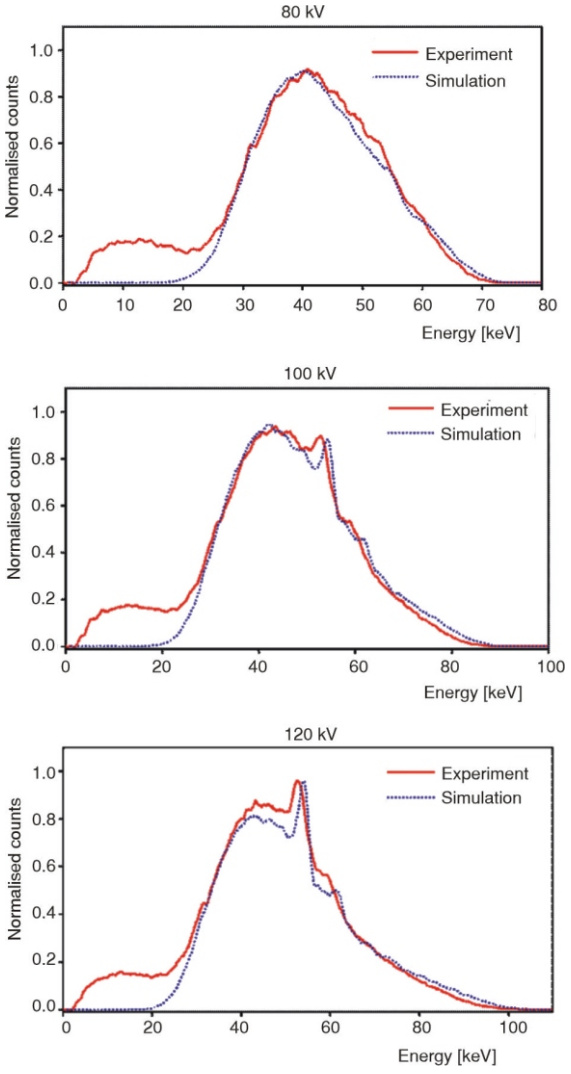

Figure 4. Comparison of the measured and simulated scattering energy spectrum at 30 cm

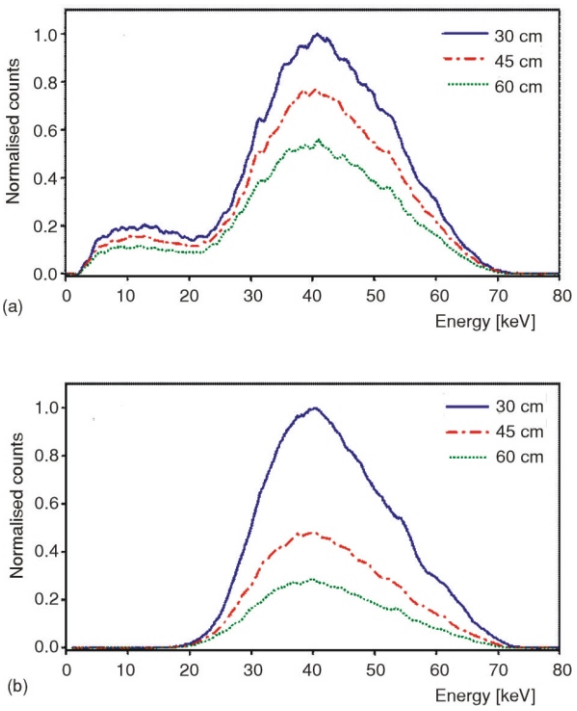

Figure 5. Scattering energy spectrum for varying spectrometer distance under 80 kV; (a) measured spectra normalized to maximum counts obtained at 30 cm and (b) simulated spectra normalized to maximum counts obtained at 30 cm

measurement and simulated energy spectrum at 30 cm from the center of the water phantom.

Figure 5 shows the measured and simulated scattering energy spectrum at a tube voltage of 80 kV. In fig. 5, the scattering energy spectrum trends are roughly the same at different distances. However, the energy spectrum counts decrease with the increase of the measurement distance. The counts of the measured energy spectrum decreased by 23 % and 44 % at distances of 45 cm and 60 cm, respectively, and the counts of the simulated energy spectrum decreased by 51 % and 71 %, respectively. The results show that the number of scattered photons will decrease rapidly with the increase of measurement distance.

The measured scattering energy spectrum is affected by the L-series characteristic peaks of tungsten, and the calculated average energy of the energy spectrum will have a large error. The distortion of the measured energy spectrum needs to be processed to reduce the error. The average energy of the processed measured and simulated energy spectrum was compared as summarized in tab. 1. The average energy calculated from the measured and simulated energy spectrum was in good agreement, and the maximum relative deviation was 2.44 %. It can be seen from the table that the average energy of the measured and simulated energy spectrum varies less with the increase of measurement distance at the same voltage. The average energy of the energy spectrum increases with the increase of the tube voltage at the same measurement position, and compared with the tube voltage 80 kV, the average energy of the tube voltage 120 kV and 100 kV increases by about 11 % and 19 %, respectively.

Scattered radiation dose measurement results

Medical staff are exposed to scattered radiation from patients during diagnostic radiology, and may receive potentially harmful radiation doses. Therefore, it is very important to evaluate and measure the scattered radiation exposure of medical staff [20-23]. At the same time, the evaluation and measurement results are also helpful increasing awareness of radiation exposure prevention of medical staff. We obtained the scattered radiation doses at different distances and angles around the water phantom. The measurement results show that when the water phantom is closer to the ionization chamber, and the corresponding measured charge was larger, that is, the scattered radiation dose was large. The charge increases with the increase of the scattering angle at the same measurement distance.

Figure 6 shows the variation trend of the charge measured with the change of the measurement dis-

Table 1. Comparison of average energy of measured and simulated scattering spectra at a 90° scattering angle

Distance from the phantom [cm]	Tube voltage [kV]	Angle of scattered radiation [90°]		
		Mean energy [keV]		Relative deviation [%]
		Experiment	Simulation	
30	80	43.22	43.09	–0.32
45	80	42.00	42.66	1.59
60	80	41.73	42.49	1.84
30	100	47.34	47.67	0.68
45	100	46.91	47.25	0.72
60	100	46.56	46.99	0.92
30	120	49.96	51.13	2.34
45	120	49.73	50.64	1.83
60	120	49.37	50.57	2.44

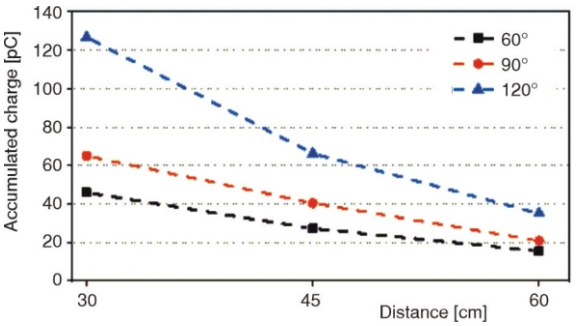

Figure 6. Accumulated charges for different scattering angles under 80 kV

tance at the tube voltage of 80 kV and the same scattering angle direction. The change trend of charge at tube voltages of 100 kV and 120 kV is the same as that of 80 kV. The measurement results indicate that the charge decreases significantly with the increase of the measurement distance. The charge amount measured at 45 cm and 60 cm distances decreased by about 52 % and 68 %, respectively, compared with those at 30 cm distances in the direction of 60°. It is reduced by about 42 % and 68 %, respectively, in the direction of 90° and by about 48 % and 72 %, respectively, in the direction of 120°. This is consistent with the results of Dorman *et al*. [24] who found that the measured scattered radiation is a non-strict inversely proportional to the distance from the radiation source. Therefore, it is very important for medical staff to maintain sufficient distance from patients during the radiological diagnosis, which can greatly reduce the scattered radiation exposure of medical staff.

Figure 7 shows the variation trend of charge with the change of the scattering angle at the tube voltage of 80 kV and the same measurement distance. The change trend of charge at tube voltages of 100 kV and 120 kV is the same as that of 80 kV. The measured charge was higher with the approaches one side of the X-ray tube of the scattering angle direction, that is, the charge increases with the increase of the scattering angle. The charge at the 120° scattering angle was generally 1 to 2 times higher than that at the 60° angle direction, indicating that the scattered radiation exposure is higher on the side closer to the X-ray tube. Normally, the X-ray tube is located below the patient's recliner during most diagnostic treatments, because this can reduce the radiation exposure to the eye lens and other sensitive organs of the medical staff. Nevertheless, the eye lens and upper body are still exposed to significant scattered radiation [25, 26]. Therefore, protective measurements are very important for medical staff, and it is necessary to wear radiation protection tools such as protective clothing and lead glasses.

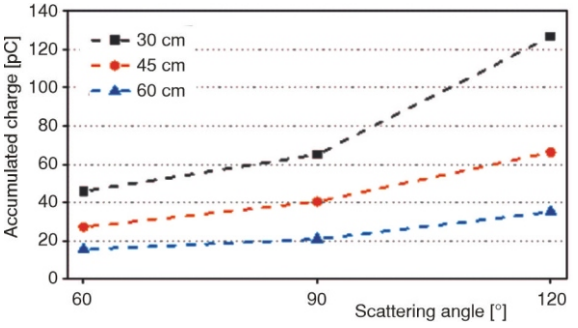

Figure 7. Accumulated charge for different measurement distances under 80 kV

Simulation results of the scattering energy spectrum at different angles, distances and tube voltages

Monte Carlo simulation is used to obtain the scattering energy spectrum information at different angles, distances and tube voltages, which is helpful to evaluate the average energy and radiation exposure of scattered X-rays that medical staff may be exposed to during practice. The energy distribution of photons in the scattering energy spectrum is a combination of both attenuation and scattering properties of incident X-rays in the water phantom. The variation of the energy spectrum between the incident energy spectrum and the scattering energy spectrum are mainly affected by two effects. The first effect is Compton scattering, where the incident photons are scattered to a lower energy, thereby reducing the average energy of the energy spectrum. The second effect is the photoelectric effect, the low-energy scattered photons are absorbed during the process of reaching the surface from the interior of the water phantom, leading to the transfer of average energy to high energy [9, 10]. The proportion of these two effects depends on the applied tube voltage and the considered scattering angle.

By comparing the average energy of the incident X-ray energy spectrum and the energy spectrum of different scattering angles, it is found that the average energy of the scattering energy spectrum at the scattering angle of 45° and 60° is generally transferred to higher energy except that the average energy of the scattering spectrum and the incident spectrum is not much different at the tube voltage of 120 kV and the scattering angle of 60°. The average energy of the scattering energy spectrum is generally lower than that of the incident energy spectrum at the scattering angles of 120° and 135°. Table 2 showed the average energy of the scattering energy spectrum and the incident energy spectrum at 100 cm from the center of the water phantom.

Figure 8 shows the variation trend of the average energy with the increase of the scattering angle at the same voltage and the measurement distance. The change trend of average energy at tube voltages of 100 kV and 120 kV is the same as that of 80 kV. The

Table 2. Average energy of scattering and incident energy spectrum at 100 cm

Tube voltage [kV]	Mean energy [keV]					
	Primary beams	Angle of scattered radiation [°]				
		45	60	90	120	135
80	42.30	45.79	44.89	42.29	39.95	39.30
100	48.40	51.03	50.00	46.84	44.24	43.39
120	53.54	55.25	53.22	50.40	47.46	46.49

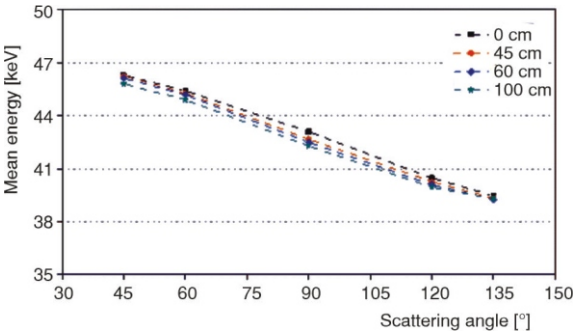

Figure 8. Average energy of simulated scattered spectra under 80 kV

average energy of the scattering energy spectrum gradually decreases with the increase of the scattering angle at the same voltage and distance, and the decreasing trend is almost consistent. Compared with the scattering angle of 45°, the average energy in the scattering angles of 90° and 135° is reduced by about 8 % and 15 %, respectively. The average energy of the scattering energy spectrum changes little with the increase of the measurement distance at the same angle and voltage, and the maximum change of the average energy between the detection distance of 30 cm to 100 cm is 0.81 keV. The average energy of the scattering energy spectrum increases with the increase of the tube voltage at the same measurement position. Compared with the tube voltage of 80 kV, the average energy in the tube voltage of 100 kV and 120 kV is increased about 11 % and 19 %, respectively. Table 3 shows the simulated average scattering energy.

Figure 9 shows the average energy of the scattering energy spectrum measured under different experiments. The measurement results at a tube voltage of 80 kV in this experiment are consistent with those of Fehrenbacher *et al.* [8] and Nowak *et al*. [27]. The average energy gradually decreased with the increase of the scattering angle at the three experiments, and the decreasing trend is almost the same. However, the conditions for measuring voltage and distance are not completely the same in each experiment, and there will be some differences in the average energy of the same scattering angle.

Figure 10 shows the ionizing radiation levels around the water phantom at a tube voltage of 80 kV. Figure 11 shows the scattering energy spectrum measured at the different scattering angles at the tube voltage of 80 kV. The ionizing radiation level distribution and the change of scattering energy spectrum at tube voltages 100 kV and 120 kV are similar to those at 80 kV.

Figures 10 and 11 show that the scattered radiation exposure is higher with the larger scattering angle or closer to the water phantom. At the same tube voltage, the photon number of the scattering energy spectrum at the measurement distance of 100 cm is approximately 90 % lower than that of 30 cm, and the number of photons in the scattering angle 135° direction is generally two to three times higher than that in the direction of 45°. This indicates the non-uniform distribution of scattered radiation around the water phantom. Therefore, if the dose in one direction of scattering is used to represent the dose in the other directions, there will be a high probability that the dose in the other directions will be incorrectly estimated. This means that different parts of the body should wear different dosemeters, the article of Nowak *et al*. [27] shows that special dosemeters are recommended for better monitoring of different parts of the body.

Table 3. Average energy of the scattered spectra for different angles

Distance from the phantom [cm]	Tube voltage [kV]	Mean energy [keV]				
		Angle of scattered radiation [°]				
		45	60	90	120	135
30	80	46.28	45.40	43.09	40.47	39.47
45	80	46.24	45.25	42.66	40.26	39.33
60	80	46.11	45.17	42.49	40.08	39.26
100	80	45.79	44.89	42.29	39.95	39.30
30	100	51.41	50.26	47.67	44.79	43.66
45	100	51.43	50.10	47.25	44.53	43.53
60	100	51.32	49.99	46.99	44.34	43.48
100	100	51.03	50.00	46.68	44.24	43.39
30	120	55.48	53.37	51.09	48.04	46.80
45	120	55.65	53.25	50.63	47.75	46.70
60	120	55.44	53.25	50.56	47.66	46.65
100	120	55.25	53.22	50.40	47.46	46.49

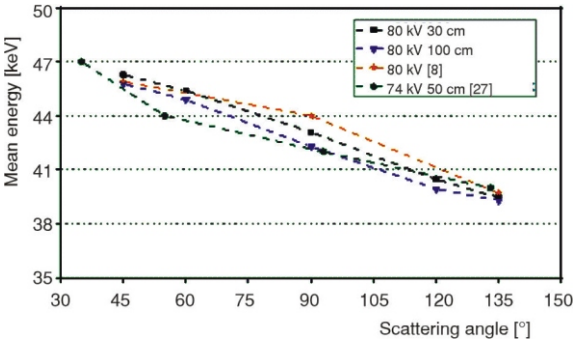

Figure 9. Comparison of average energy under different conditions

Figures 10 and 11 show that the distribution of photon fluence at different scattering angles is more uniform when the distance from the center of the water model is 100 cm. This indicates that the dose results for a particular scattering angle direction can be used to replace the dose results for other parts of the body only when the medical staff is more than 100 cm away from the patient generating the radiation field.

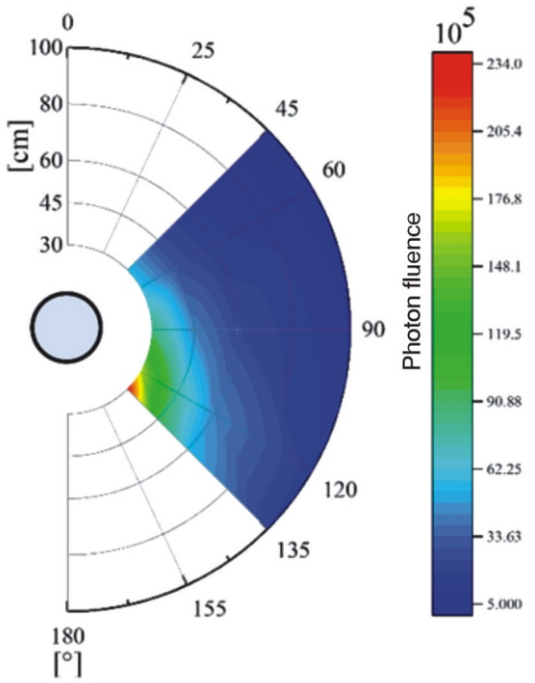

Figure 10. Photon fluence distribution map for the different scattering angles under 80 kV

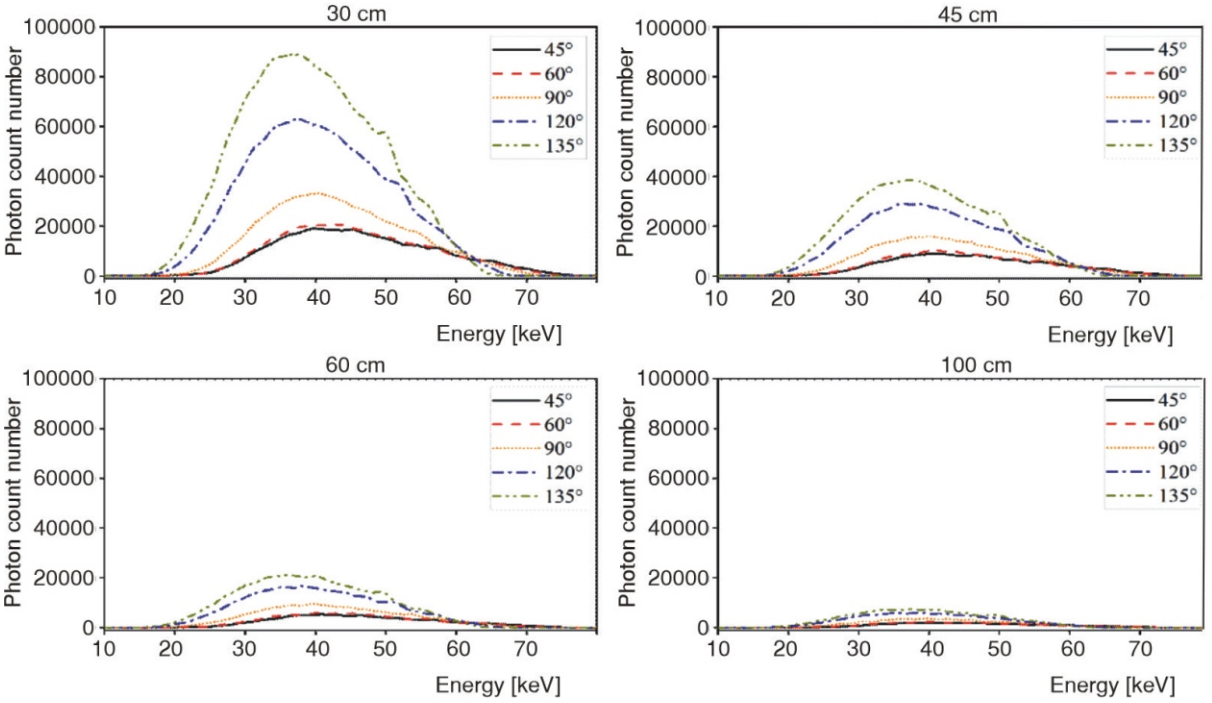

Figure 11. Scatter energy spectrum for varying spectrometer distance under 80 kV

CONCLUSIONS

This article obtains the diagnostic X-ray scattered radiation energy spectrum and dose distribution under tube voltage of 80 kV, 100 kV, and 120 kV through Monte Carlo simulation and experimental measurement. The average energy and trend of the measured and simulated energy spectrum are in good agreement at the scattering angle of 90°, and the relative deviation is less than 2.44 %, which indicates the correctness of the established detection scattering energy spectrum model. The average energy of the en-

ergy spectrum increases with the increase of the tube voltage at the same measurement position. The average energy of the scattering energy spectrum gradually decreases with the increase of the scattering angle at the same voltage and measurement distance. The average energy of the scattering energy spectrum changes little with the increase of the measurement distance at the same angle and voltage, and the maximum change of the average energy between different measurement distances is 0.81 keV. The radiation field around the water phantom is characterized by the measured scattering dose and the simulated scattering energy spectrum, and the results showed that the radiation exposure around the water phantom was not unified. The measured scattering dose indicates that the charge at a measurement distance of 60 cm is approximately 70 % lower than that at 30 cm. The number of photons in the scattering angle 135° direction is generally two to three times higher than that in the direction of 45°, and this indicates that the exposure to scattered radiation was greater on the side closer to the water phantom or the X-ray tube. This study provides an estimate of the scattered radiation exposure of medical staff in practice and enhances the self-protection awareness of medical staff, and reduces the scattered radiation exposure of medical staff.

AUTHORS' CONTRIBUTIONS

X. Tang: Methodology, software, investigation, writing – original draft. R. Zhao: Supervision, writing – review and editing. W. Zhu: Writing – review and editing. B. Guo: Resources, funding. J. Wu: Supervision, review, resources, acquisition. F. Qin: Investigation, resources. B. Liu: Formal analysis.

ACKNOWLEDGMENT

This work has been supported by the project of NIM (ANL2210).

REFERENCES

[1] Bhargavan, M., Trends in the Utilization of Medical Procedures that Use Ionizing Radiation, *Health Phys, 95* (2008), 5, pp. 612-627
[2] Mettler, F. A. J., *et al*., Radiologic and Nuclear Medicine Studies in the United States and Worldwide: Frequency, Radiation Dose, and Comparison with Other Radiation Sources 1950-2007, *Radiology, 253* (2009), 2, pp. 520-531
[3] Rajaraman, P., *et al*., Cancer Risks in U.S. Radiologic Technologists Working With Fluoroscopically Guided Interventional Procedures, 1994-2008, *Am J Roentgenol, 206* (2016), 5, pp. 1101-1110
[4] ***, International Commission on Radiological Protection, Statement on Tissue Reactions: 2011
[5] Seals, K. F., *et al*., Radiation-Induced Cataractogenesis: A Critical Literature Review for the Interventional Radiologist, *Cardiovasc Intervent Radiol, 39* (2016), 2, pp. 151-160
[6] Sanchez, R. M., *et al*., Staff Doses in Interventional Radiology: a National Survey, *J Vasc Interv Radiol, 23* (2012), 11, pp. 1496-1501
[7] Marshall, N. W., *et al*., Measured Scattered X-Ray Energy Spectra for Simulated Irradiation Geometries in Diagnostic Radiology, *Med Phys, 23* (1996), 7, pp. 1271-1276
[8] Fehrenbacher, G., *et al*., Determination of Diagnostic X Ray Spectra Scattered by a Phantom, *Radiat Prot Dosimetry, 71* (1997), 4, pp. 305-308
[9] Masterson, M., *et al*., Relative Response of Dosimeters to Variations in Scattered X-Ray Energy Spectra Encountered in Interventional Radiology, *Phys Med, 67* (2019), Nov., pp. 141-147
[10] Williams, J. R., The Interdependence of Staff and Patient Doses in Interventional Radiology, *Br J Radiol, 70* (1997), 833, pp. 498-503
[11] Chida, K., *et al*., Physician-Received Scatter Radiation with Angiography Systems Used for Interventional Radiology: Comparison Among Many X-Ray Systems, *Radiat Prot Dosimetry, 149* (2012), 4, pp. 410-416
[12] Antić, V. M., Semi-Automatic Positioning of the Protective Screen Based on Integration with C-Arm X-Ray Device, *Nucl Tecnol Radiat, 36* (2021), 1, pp. 85-90
[13] Bordy, J. M., *et al*., Principles for the Design and Calibration of Radiation Protection Dosemeters for Operational and Protection Quantities for Eye Lens Dosimetry, *Radiat Prot Dosimetry, 144* (2011), 1-4, pp. 257-261
[14] Rahman, Z., *et al*., Geant4-Based Comprehensive Study of the Absorbed Fraction for Electrons and Gamma-Photons Using Various Geometrical Models and Biological Tissues, *Nucl Tecnol Radiat, 28* (2013), 4, pp. 341-351
[15] Arectout, A., *et al*., Calculation of X-Ray Spectra Characteristics and Kerma to Personal Dose Equivalent Hp(10) Conversion Coefficients: Experimental Approach and Monte Carlo Modeling, *Nuclear Engineering and Technology, 54* (2022), 1, pp. 301-309
[16] Zhao, R., *et al*., The Establishment of Radiation Qualities and Energy Spectra Simulation of X-Ray Lead Equivalent Measurement, *Acta Metrologica Sinica, 43* (2022), 7, pp. 960-964
[17] Kodera, Y., *et al.*, Effect of Collimators on the Measurement of Diagnostic X-Ray Spectra, *Phys Med Biol, 28* (1983), 7, pp. 841-852
[18] Dick, C. E., *et al.*, X-Ray Scatter Data for Diagnostic Radiology, *Phys Med Biol, 23* (1978), 6, pp. 1076-1085
[19] Usman, S., Patil, A., Radiation Detector Dead Time and Pile Up: A Review of the Status of Science, *Nuclear Engineering and Technology, 50* (2018), 7, pp. 1006-1016
[20] Ishii, H., *et al.*, Occupational Eye Dose Correlation with Neck Dose and Patient-Related Quantities in interventional Cardiology Procedures, *Radiol Phys Technol, 15* (2022), 1, pp. 54-62
[21] Inaba, Y., *et al*., Fundamental Study of a Real-Time Occupational Dosimetry System for interventional Radiology Staff, *J Radiol Prot, 34* (2014), 3, pp. 65-71
[22] Chida, K., *et al*., Effect of Radiation Monitoring Method and Formula Differences on Estimated Physician Dose During percutaneous Coronary Intervention, *Acta Radiol, 50* (2009), 2, pp. 170-173
[23] Morishima, Y., e*t al*., The Effectiveness of Additional Lead-Shielding Drape and Low Pulse Rate Fluoroscopy in Protecting Staff from Scatter Radiation During Cardiac resynchronization Therapy (CRT), *Jpn J Radiol, 37* (2019), 1, pp. 95-101

[24] Dorman, T., *et al*., Radiation Dose to Staff from Medical X-Ray Scatter in the Orthopaedic Theatre, *Eur J Orthop Surg Traumatol, 33* (2023), 7, pp. 3059-3065
[25] Leyton, F., *et al*., Correlation Between Scatter Radiation Dose at Height of Operator's Eye and Dose to Patient for Different angiographic Projections, *Appl Radiat Isot, 117* (2016), Nov., pp. 100-105
[26] Leyton, F., *et al*., Scatter Radiation Dose at the Height of the Operator's Eye in interventional Cardiology, *Radiation Measurements, 71* (2014), Dec., pp. 349-354
[27] Nowak, M., *et al*., Characterisation and Mapping of Scattered Radiation Fields in interventional Radiology Theatres, *Sci Rep,10* (2020), 1, pp. 18754

Received on July 19, 2023
Accepted on October 16, 2023

Сјен ЋАНГ ТАНГ, Жуеј ЦАО, Веј ФЕНГ ЦУ, Бин ГУО, Фенг ЋИН, Бо ЉУ, Ћин ЂЕ ВУ

СИМУЛАЦИЈА И МЕРЕЊЕ РАСЕЈАНОГ РЕНДГЕНСКОГ ЗРАЧЕЊА У РАДИОДИЈАГНОСТИЦИ

Овај рад има за циљ мерење енергетског спектра расејаног зрачења и дозе зрачења на различитим позицијама током радиолошке дијагнозе, коришћењем Монте Карло симулације и експеримената. Резултати показују да просечна енергија спектра енергије расејаног зрачења расте са порастом напона цеви и опада са повећањем угла расејања, али се врло мало мења са растојањем мерења. Такође, расподела расејаног зрачења није уравнотежена у простору око воденог фантома при истом напону цеви, а изложеност расејаном зрачењу је већа на страни ближе воденом фантому или рендгенској цеви. Ово указује да изложеност зрачењу није јединствена за медицинско особље у пољу расејаног зрачења. Енергетски спектар расејања и расподела дозе помажу у процени изложености расејаном зрачењу и повећавају свест медицинског особља о самозаштити у ординацији.

Кључне речи: радиодијагностика Х-зрачењем, расејано зрачење, Монте Карло, енергетски спектар, излагање зрачењу.